RESEARCH ARTICLE
doi: 10.2306/scienceasia1513-1874.2021.049

ScienceAsia 47 (2021): **340–346**

Localized surface plasmon resonance for improving optical absorption in core-shell Ag@TiO_2 nanoparticles

Supachai Sompech[a,b], Pongsak Jittabut[c], Sukhontip Thaomola[d], Sasiporn Audtarat[a,b], Panadda Charee[a], Thananchai Dasri[a,b,*]

[a] Faculty of Interdisciplinary Studies, Khon Kaen University, Nong Khai Campus, Nong Khai 43000 Thailand
[b] Integration Research Unit for Energy and Environment, Khon Kaen University, Nong Khai Campus, Nong Khai 43000 Thailand
[c] Physics and General Science Program, Faculty of Science and Technology, Nakhon Ratchasima Rajabhat University, Nakhon Ratchasima 30000 Thailand
[d] Faculty of Science and Arts, Burapha University, Chanthaburi Campus, Chanthaburi 22170 Thailand

[*]Corresponding author, e-mail: thananchai@kku.ac.th

Received 6 Jun 2020
Accepted 25 Apr 2021

ABSTRACT: Titanium dioxide (TiO_2) has attracted extensive attention in environmental and biomedical applications, owing to its excellent chemical and photochemical stabilities, non-toxicity, and high degradation capacity. However, the wide band gap and low quantum yield of TiO_2 limit its practical applications, and it is possible to improve the optical efficiency and sensitivity of TiO_2 in the visible spectrum. In this work, theoretical calculations based on optical absorption in core-shell structured Ag@TiO_2 nanoparticles (NPs) combined with the surface plasmon resonance property of the core and photoactivity of the shell were investigated as a function of incident light wavelengths in visible spectrum. Shifting of wavelength, at which light was absorbed and enhanced optical absorption activity of TiO_2 NPs due to localized surface plasmon resonance excitation were clearly observed at a level greatly exceeding the value calculated for pure TiO_2 NPs. The calculated results suggest that both the interparticle distance and the diameter of Ag core in the core-shell structure of Ag@TiO_2 NPs influence the tuning and the enhancement of optical absorption spectra. These findings of enhanced optical absorption could be utilized as basic knowledge to design and synthesize Ag@TiO_2 NPs for future environmental and biomedicine applications.

KEYWORDS: AgTiO_2 nanoparticles, optical absorption property, surface plasmon resonance

INTRODUCTION

Titanium dioxide (TiO_2) metal-oxide semiconducting nanomaterial is regarded as the most effective photocatalyst for energy and environmental pollution treatment applications [1–4]. Moreover, TiO_2 has been shown to be chemically inert with especially strong oxidizing power arising from photogenerated holes [5]. TiO_2 nanomaterials, i.e. nanoparticles, nanorods, nanowires, nanobelts, and nanotubes, have been utilized in numerous applications [6–9]. However, its wide band gap energy of ∼3.2 eV limits its potential applications in the visible range of light irradiation. Additionally, sunlight is largely comprised of visible light. Therefore, the photocatalytic activities of TiO_2 exhibit insufficient light absorption when irradiated with sunlight due to its quick recombination of photogenerated charge carriers and the limited availability of ultraviolet (UV) light. Several techniques were proposed to make the photocatalyst reactive under visible light (λ>380 nm). Integration of TiO_2 with noble metals such as gold (Au) and silver (Ag), among others, has been shown an effective approach to improve its photocatalytic activity in terms of its localized surface plasmon resonance (LSPR) properties [10–12]. The LSPR effects can contribute to more effective light harvesting by expanding the optical absorption range from the UV to visible wavelengths of light. In the current study, the light absorption of TiO_2 integrated with Ag nanoparticle, henceforth referred to as Ag@TiO_2 core-shell NPs, was numerically calculated using a discrete dipole approximation (DDA) technique. The relationship between the spectral absorption characteristics, TiO_2 shell thickness, and interparticle distance of Ag@TiO_2 core-shell NPs at wavelengths between 300–900 nm were provided by computational analysis. These findings

of enhanced optical absorption activity could be utilized to design and synthesize Ag@TiO_2 core-shell NPs with desirable photocatalytic and antimicrobial activities for future environmental and biomedical applications.

METHODS

Thoretical calculations

DDA is numerical method for calculating the optical properties (extinction, scattering, and absorption cross sections) of target materials, and it is subdivided into N point dipoles [7]. According to this approach, the optical absorption property of the whole structure can be precisely calculated when the coordinates and polarizabilities of the individual dipoles are known. When the dipole located at a point r_j is induced by an incident electric field, it generates an associated electric field called dipole moment, given by Eq. (1):

$$P_j = \tilde{a}_j E_{\text{loc}}(r_j), \tag{1}$$

where $\tilde{a}_j$ is polarizability tensor of this dipole, $E_{\text{loc}}(r_i)$ is the induced field at a dipole located at r_i due to the incident field $E_{\text{inc}}(r_i)$, and the field emitted by all neighboring $N-1$ dipoles P_j, shown as Eq. (2),

$$E_{\text{loc}}(r_i) = E_{\text{inc}}(r_i) - \sum_{i \neq j} \widetilde{A}_{ij} P_j, \tag{2}$$

where for $i \neq j$,

$$\widetilde{A}_{ij} = \frac{e^{ikr_{ij}}}{r_{ij}} \left[k^2(\hat{r}_{ij}\hat{r}_{ij} - I_3) + \frac{ikr_{ij}-1}{r_{ij}^2}(3\hat{r}_{ij}\hat{r}_{ij} - I_3) \right], \tag{3}$$

where $k = 2\pi n_m/\lambda$ (where λ and n_m are the wavelength of light and the refractive index of the incident medium, respectively), $\hat{r}_{ij} = (r_i - r_j)/r_{ij}$ is the unit vector along r_{ij} (where $r_{ij} = |r_i - r_j|$, and I_3 is an identity matrix of 3×3. If $i = j$, self-interaction $\widetilde{A}_{ii}$ in Eq. (3) is given by: $\widetilde{A}_{ii} = \alpha_i^{-1}$, where α_i is the polarizability of dipole calculated by using Kuwata's approximation [8] in Eq. (4):

$$\alpha_i = \frac{V}{(L + \frac{\varepsilon_m}{\varepsilon_i - \varepsilon_m}) + A\varepsilon_m x^2 + B\varepsilon_m^2 x^4 - i_i \frac{4\pi^2 \varepsilon_m^{1.5}}{3} \frac{V}{\lambda^3}}. \tag{4}$$

Here, $L = 1/3$ for a spherical shape, V and x are the volume and a size parameter of particle, respectively. ε_i and ε_m are the dielectric functions of particle and the surrounding medium matrix, respectively. The parameters of A and B are defined as:

$$A(L) = -0.4865L - 1.046L^2 + 0.8481L^3,$$
$$B(L) = 0.01909L + 0.1999L^2 + 0.6077L^3.$$

$\widetilde{A}_{ij}$ describes the dipole-dipole interaction between a receiving dipole at r_i and a radiating dipole at r_j. These form a $3N \times 3N$ block diagonal matrix consisting of the inverses of the 3×3 polarizability matrices of the N dipoles. The polarization of each particle P_i can be calculated by solving a linear system of $3N$ equations. This leads to the absorption cross section as shown in Eq. (5):

$$C_{\text{abs}} = \frac{4\pi k}{|E_0^2|^2} \sum_{i=1}^{n} \left[\text{Im}(P_i \cdot (\alpha_i^{-1})^* P_i)^* - \frac{2}{3} k^3 |P_i|^2 \right], \tag{5}$$

where the asterisk (*) is the conjugate of a complex variable. E_0 defines as the amplitude of the incident electric field. Q_{abs} is the absorption efficiency ($Q_{\text{abs}} = C_{\text{abs}}/\pi R^2$, R is the radius of a spherical NP). For core-shell NPs, $\varepsilon_i = \varepsilon_{\text{cs}}$ in Eq. (4) can be obtained by Eq. (6) according to [13, 14]:

$$\varepsilon_{\text{cs}} = \varepsilon_{\text{sh}} \frac{1 + 2\beta_{\text{cs}}}{(1 - \beta_{\text{cs}})}, \tag{6}$$

where $\beta_{\text{cs}} = (\frac{R_c}{R_{\text{sh}}})^3 (\frac{\varepsilon_c - \varepsilon_{\text{sh}}}{\varepsilon_c + 2\varepsilon_{\text{sh}}})$, ε_{sh} and ε_c are the dielectric constant of the shell and the core, respectively. R_c and R_{sh} are the radii of the core and the shell of the particle as denoted in Fig. 1a, respectively. The dielectric constant for TiO_2 has been published [15] as the dielectric constant for Ag [16]. The core's diameter and the shell thickness of Ag@TiO_2 NP were taken following Ref. [17]. The core-shell NP was assumed to be surrounded by a homogeneous medium of water ($\varepsilon_m = 1.69$), which relates to surrounding environment application of Ag@TiO_2 such as anticancer modality photocatalytic and photothermal cell killing under solar light irradiation [17]. For this calculation, the modeled samples are illustrated in Fig. 1. Fig. 1a presents a modeled core-shell composite NP and its effective sphere. Fig. 1b and Fig. 1c depict two NPs consisting of pure Ag and Ag@TiO_2 core shell, respectively.

RESULTS AND DISCUSSION

Initially, the optical absorption activity obtained by the DDA method was compared with the exact solution by Mie theory [18, 19]. Spherical NPs of single Ag with diameters of 10, 30, and 50 nm embedded in water are illustrated in Fig. 1. The results showed

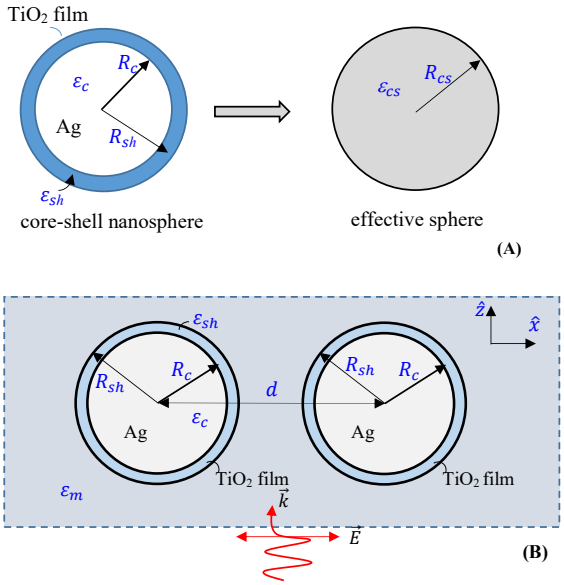

Fig. 1 Schematic drawings of (A) a core-shell nanoparticle and its effective sphere and (B) two closely spaced Ag@TiO_2 core-shell NPs. The parameters R_c and ε_c represent core radius and electrical permittivity, respectively. While R_{sh} and ε_{sh} define as radius and electrical permittivity of shell. ε_m and d represent the electrical permittivity of the host medium and interparticle distance, respectively. The direction of the propagation and the polarization of the incident electric field are also indicated.

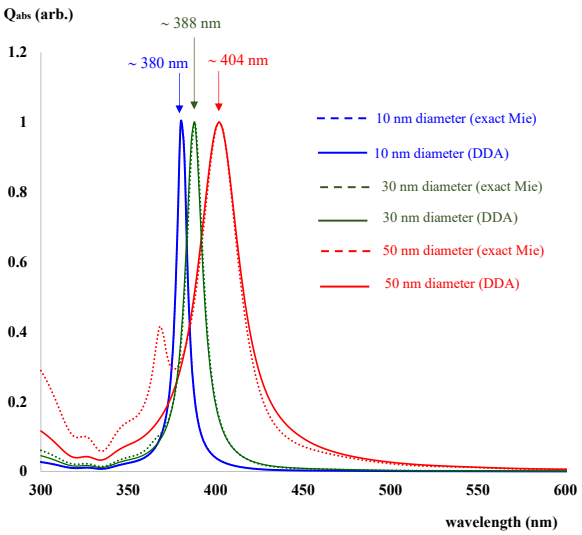

Fig. 2 Comparison of DDA with exact solution by Mie theory for single Ag nanoparticle absorption.

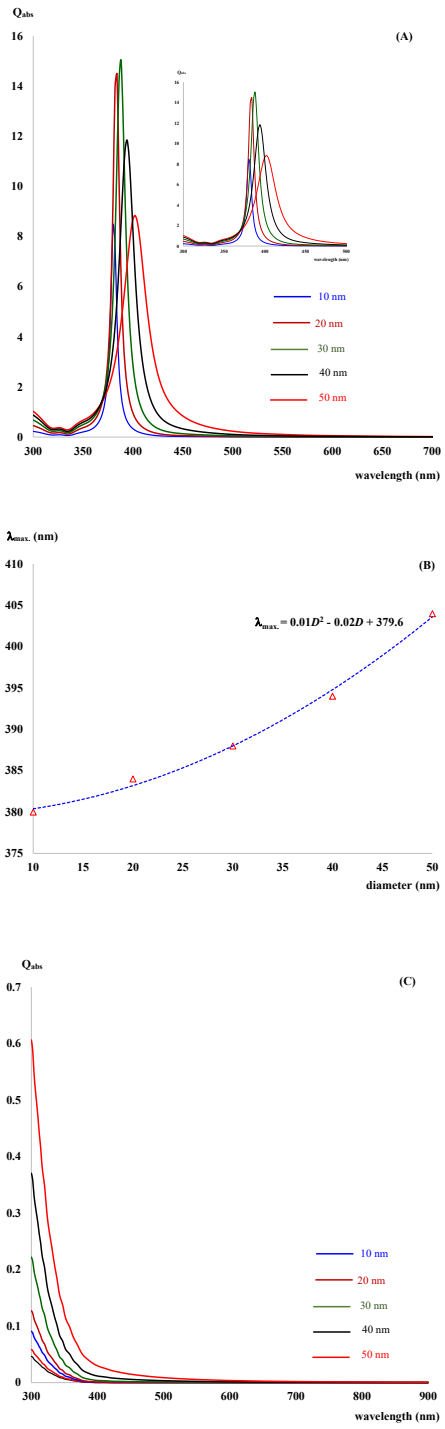

Fig. 3 Calculated absorption spectra of (A) pure Ag nanoparticles with varying diameters, (B) LSPR positions of Ag as function of the diameters, and (C) pure TiO_2 with varying diameters, embedded in water.

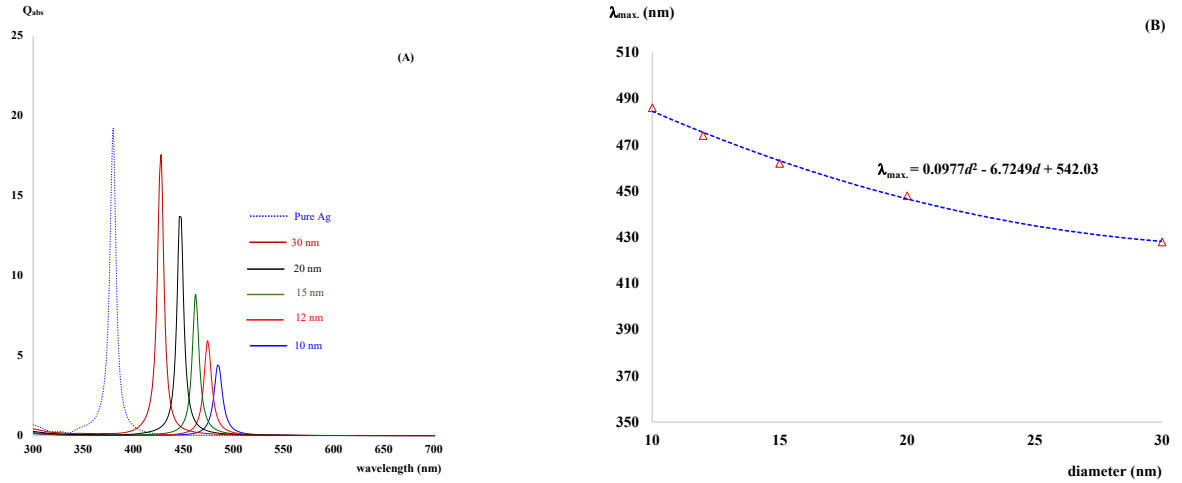

Fig. 4 Calculated (A) absorption spectra of Ag@TiO_2 composite nanoparticles with various diameters between 10–30 nm and (B) the relationship between LSPR positions and Ag core diameters. The shell thickness of TiO_2 layer was fixed at 5 nm.

that the absorption efficiency calculated by DDA method was in good agreement with the exact Mie theory [18, 19] for very small particles. Resonance absorption peaks of the 10, 30, and 50 nm diameter particles were observed at ∼380, ∼388, and ∼404 nm, respectively. The most significant departure from the exact Mie theory was observed with the larger 50 nm diameter particles. A quadrupolar mode was found in the exact Mie spectrum that appeared at a shorter wavelength compared with the dipolar mode. The quadrupolar and the dipole peaks were clearly seen at ∼368 nm and ∼404 nm, respectively (Fig. 2). Fig. 3a shows a shift of the LSPR position to a longer wavelength due to the varying sizes of the Ag NPs. It was observed that the relationship between LSPR position (λ_{max}) and Ag diameter (D) was second degree polynomial, $\lambda_{max} = 0.01D^2 - 0.02D + 379.6$ (Fig. 3b). The shift of LSPR peak position can be explained from the plasmon hybridization theory [20, 21]. The solid sphere plasmon resonance, ω_{LSPR}, can be found as $\omega_{LSPR} = \omega_p(l/2l+1)^{0.5}$, where l refers to the spherical harmonic order; bulk plasmon frequency (ω_p) is defined by $\omega_p = (Ne^2/m^*\varepsilon_0)^{0.5}$, where ε_0 is the permittivity of vacuum; m^* and e are the effective mass and charge of an electron, respectively; and N is the bulk charge density. Therefore, when the particle size is large enough, the electron cloud experiences increasing depolarization and higher multipoles, especially the quadrupolar ($l = 2$), damping the electron oscillation to lower energies or redshift. It is clear that Ag NPs show a strong LSPR signal characteristic leading to increased light absorption in the visible light region of electromagnetic spectrum. Alternatively, the absorption spectra at various TiO_2 diameters show absorption peaks outside of the visible region and produce low intensity optical absorption (Fig. 3c), which are in agreement with the reported results [17]. Therefore, by integrating with plasmonic NPs (such as Ag NPs), the optical properties of TiO_2 should be improved as reported [17]. Firstly, an isolated composite NP of Ag coated with a TiO_2 nanolayer (Fig. 1a) was used to characterize the optical absorption properties. Fig. 4 shows absorption spectra of Ag@TiO_2 composite NPs with shell thickness of TiO_2 layer fixed at 5 nm. The diameters of the Ag core NPs were varied from 10 to 30 nm. The calculated results show that there is an increase of light absorption in the visible domain of the electromagnetic spectrum (Fig. 4a), which is due to the influence of Ag NPs [17]. Moreover, based on the analysis of plasmonic hybridization model, which is analogous to the molecular orbital theory [20, 21], the LSPR position of the core-shell structure also depends upon the shell thickness [22]. The LSPR hybridization in core-shell NPs can be described by the interaction between the inner and outer shell resonances. The increased shell thickness leads to a weaker coupling between the inner and outer plasmons. As the NP sizes increase, the higher-order modes, such as the quadrupolar mode where half of the electron cloud moveing parallel to the electric field and the other half anti-parallel, become important to damp the

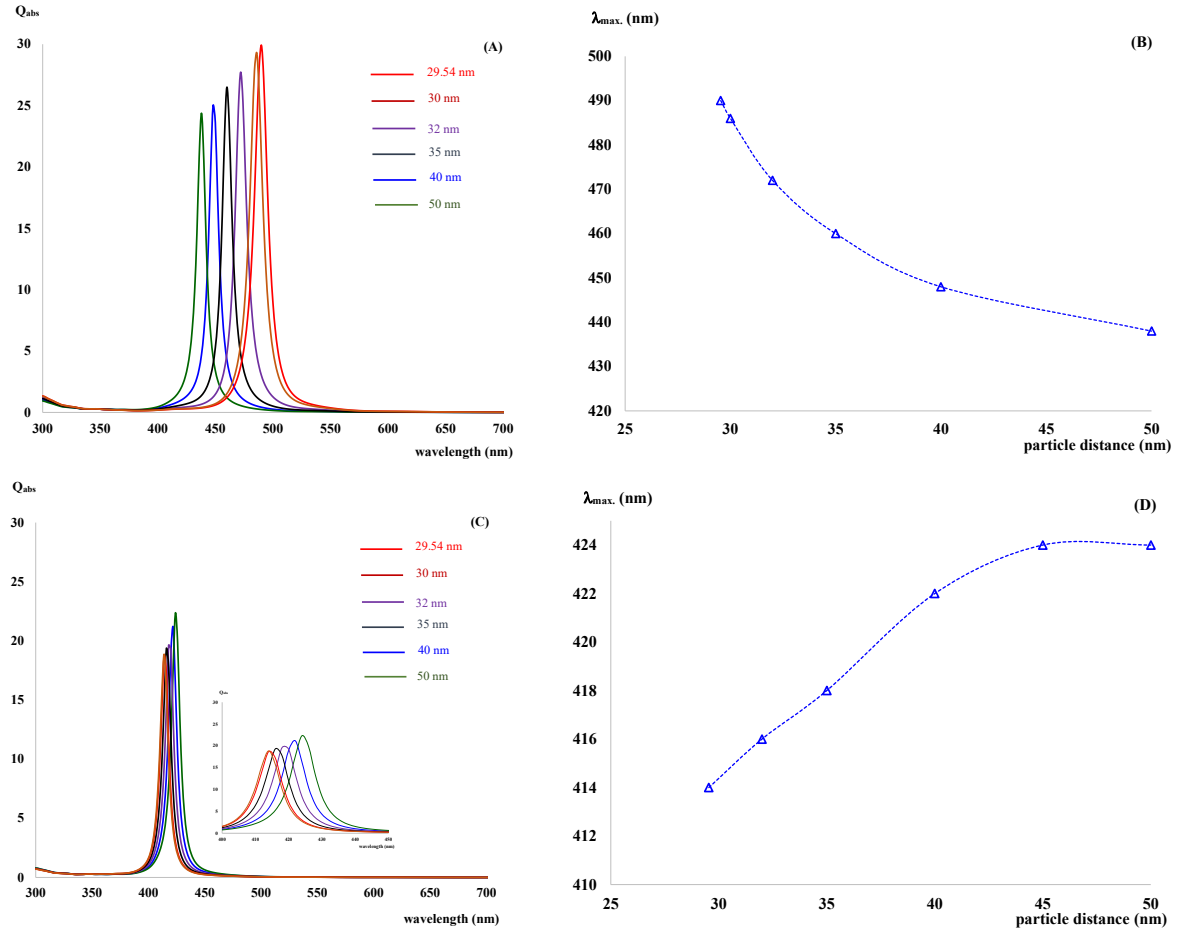

Fig. 5 Calculated absorption spectra of Ag@TiO_2 (fixed 30 nm diameter and 5 nm shell thickness) composite NPs with varying interparticle distances between 29.54–50 nm: (A) and (B) particle axis parallel to the polarization direction and perpendicular to the propagation direction of incident light, and (C) and (D) particle axis perpendicular to both polarization and propagation directions of incident light.

electron oscillation to lower energies. As a result, the LSPR position exhibits a redshift with increasing TiO_2 shell thickness under light illumination. The best fit between LSPR position (λ_{max}) and Ag core diameter (d) is given by a second order polynomial, $\lambda_{max} = 0.0977d^2 - 6.7249d + 542.03$ (Fig. 4b). Next, the influences of interparticle distance between NPs and the polarization direction on optical absorption were investigated. The fabricated Ag@TiO_2 core-shell NP samples and the interaction between NPs and incident light are illustrated in Fig. 1a and Fig. 1b, respectively. In the first case, the particle axis was aligned parallel to the direction of polarization and orthogonal to propagation direction of incident light. As the interparticle distances decreased from 50 to 29.54 nm, the LSPR positions became progressively red-shifted (Fig. 5a). Red-shifting was clearly seen when the LSPR positions from Fig. 5a were plotted as function of incident wavelengths (Fig. 5b). In the contrary, other geometries showed blue-shifting of the LSPR positions with decreasing interparticle distances when the direction between two particles was orthogonal to both the polarization and propagation directions of incident light (Fig. 5c). By plotting the LSPR positions as function of incident wavelengths, a decrease in the LSPR positions with decreasing interparticle distances was clearly observed (Fig. 5d). Based on the dipole-dipole coupling model [20, 21] for polarization direction dependent behavior of the LSPR shift resulting from the presence of an electric field derived from incident light, each particle produces electric charges along those surfaces with repulsive forces. Therefore, in the case when the direction

of polarization of electric field is parallel to the direction of the longer axis of these particles, a weakening of the repulsive forces of the surface charges is generated. Consequently, a decreased resonance frequency is found. On the other hand, when the polarization direction of electric field is perpendicular to the particles' axis direction, the charge distributions of both particles act cooperatively, and the repulsive action of the two particles are enhanced. Thus, an increasing of the resonance frequency is induced. Additionally, the metallic shell thickness of the nanostructured core-shell particles also determines the LSPR position associated with the strength of plasmon interaction [20, 21]. Two new LSPRs for antisymmetric and symmetric plasmons modes are generated by coupling metallic sphere plasmons with cavity plasmons possessed by two interface systems of outer-shell surface and inner-shell surface spheres, respectively. The antisymmetric coupling results in a higher frequency mode (blue-shifted), while the symmetric combination corresponds to a lower frequency mode (red-shifted). The coupling energy is geometrically proportional to the ratio between the inner and outer radii of the metallic shell. This means that the metallic shell thickness is associated with the strength of plasmon interaction. Environmental applications of TiO_2 NPs involve modification of TiO_2 sensitivity to visible light. The results of the current work indicate that TiO_2@Ag core-shell structured NPs can serve as new composite materials capable of uniquely controlling optical absorption in the visible spectrum of electromagnetic radiation. Based on our results, Ag@TiO_2 core-shell structured NPs can be developed to further basic scientific knowledge and engineering fundamental optical properties giving them potentials for novel applications that are not possible with pure TiO_2.

CONCLUSION

The optical activities of core-shell Ag@TiO_2 NPs were investigated using a DDA method. The optical absorption of TiO_2 NPs can be enhanced and tuned from the UV region into the visible light region of the EM wave spectrum by integrating Ag NPs into TiO_2. These properties are strongly dependent on the diameter of Ag core, interparticle distance of Ag@TiO_2 NPs, and the directions of incident light. All of the current results can be utiluzed for further study and to synthesize core-shell Ag@TiO_2 NPs to be used in future environmental applications and plasmonic devices that are not possible with pure TiO_2.

Acknowledgements: This work was financially supported from Research Program of "Development of composite biomaterials derived from agricultural by-products for applications in industry and agriculture" and Integration Research Unit for Energy and Environment by the Research and Graduate studies, Khon Kaen University. The authors acknowledge the facilities and support of the Faculty of Interdisciplinary Studies, Nong Khai Campus, Khon Kaen University.

REFERENCES

1. Prakash J, Sun S, Swart HC, Gupta RK (2018) Noble metals-TiO_2 nanocomposites: From fundamental mechanisms to photocatalysis, surface enhanced Raman scattering and antibacterial applications. *Appl Mater Today* **11**, 82–135.
2. Acosta-Mora P, Domen K, Hisatomi T, Lyu H, Méndez-Ramos J, Ruiz-Morales JC, Khaidukov NM (2018) Shifting the NIR into the UV-blue: Up-conversion boosted photocatalysis. *Opt Mater* **83**, 315–320.
3. Wan Y, Wang J, Wang X, Zu H, Yuan S, Zhang Q (2019) Preparation of inverse opal titanium dioxide for photocatalytic performance research. *Opt Mater* **96**, ID 109287.
4. Zhang B, Xu C, Xu G, Tan S, Zhang J (2019) Amorphous titanium dioxide film with improved electrochromism in near-infrared region. *Opt Mater* **89**, 191–196.
5. Zhao QE, Wen W, Xia Y, Wu JM (2018) Photocatalytic activity of TiO_2 nanorods, nanowires and nanoflowers filled with TiO_2 nanoparticles. *Thin Solid Films* **648**, 103–107.
6. Zhao Z, Tian J, Sang Y, Cabot A, Liu H (2015) Structure, synthesis, and applications of TiO_2 nanobelts. *Adv Mater* **27**, 2557–2582.
7. Purcell PM, Pennypacker CR (1973) Scattering and absorption of light by nonspherical dielectric grains. *Astrophys J* **186**, 705–714.
8. Kuwata H, Tamaru H, Esumi K, Miyano K (2003) Resonant light scattering from metal nanoparticles: Practical analysis beyond Rayleigh approximation. *Appl Phys Lett* **83**, ID 4625.
9. Hirunpinyopas W, Davis SA, Sirisaksoontorn W, Songsasen A (2015) Sm/N-codoped TiO_2 preparation, characterization, and photocatalytic decolourization of Acid Orange 7 and Basic Blue 41 in sunlight. *ScienceAsia* **41**, 42–48.
10. Sompech S, Thaomola S, Chingsungnoen A, Dasri T (2019) Theoretical calculation of optical absorption property of Cu@Ag core-shell composite nanoparticle. *Mater Res Express* **6**, ID 026201.
11. Sompech S, Thaomola S, Dasri T (2016) Optical effects in the active layer of organic solar cells with embedded noble metal nanoparticles. *Orient J Chem* **32**, 85–91.

12. Jittabut P, Seehamart K, Chingsungnoen A, Dasri T (2020) Tuning the optical and magneto-optical properties in core-shell structured Fe@Ag nanoparticles. *Adv Nat Sci Nanosci Nanotechnol* **11**, ID 045008.
13. Chettiar UK, Engheta N (2012) Internal homogenization: Effective permittivity of a coated sphere. *Opt Express* **20**, 22976–22986.
14. Chingsungnoen A, Chaiyachate P, Dasri T (2017) Composite Fe3O4@Au core-shell nanoparticle: Tunable and enhancement of optical absorption property. *Orient J Chem* **33**, 1642–1647.
15. Skowronski A, Wachowiak AA, Grabowski A (2016) Characterization of optical and microstructural properties of semitransparent TiO2/Ti/glass interference decorative coatings. *Appl Surf Sci* **388**, 731–740.
16. Johnson PB, Christy RW (1972) Optical constants of the noble metals. *Phys Rev B* **6**, ID 4370.
17. Abdulla-Al-Mamun M, Kusumoto Y, Zannat T, Islam MS (2011) Synergistic cell-killing by photocatalytic and plasmonic photothermal effects of Ag@TiO_2 core-shell composite nanoclusters against human epithelial carcinoma (HeLa) cells. *Appl Catal A Gen* **398**, 134–142.
18. Mie G (1980) Beiträge zur Optik trüber Medien, speziell kolloidaler Metalllösungen. *Ann Phys* **330**, 377–445.
19. Kreibig U (2008) Hundert Jahre Mie-Theorie. *Phys Unserer Zeit* **39**, 281–287.
20. Prodan E, Nordlander P (2003) Structural tunability of the plasmon resonances in metallic nanoshells. *Nano Lett* **3**, 543–547.
21. Prodan E, Nordlander P (2004) Plasmon hybridization in spherical nanoparticles. *J Chem Phys* **120**, 5444–5454.
22. Chen F-X, Wang X-C, Xia D-L, Wang L-S (2015) Design and optimization of Ag-dielectric core-shell nanostructures for silicon solar cells. *AIP* Advances **5**, ID 097129.